Hypophosphorylated pRb knock-in mice exhibit hallmarks of aging and vitamin C-preventable diabetes

Zhe Jiang[1, *], Huiqin Li[1], Stephanie A. Schroer[1], Veronique Voisin[2], YoungJun Ju[1], Marek Pacal[3, 4], Natalie Erdmann[5], Wei Shi[1], Philip E.D. Chung[1,4], Tao Deng[1], Nien-Jung Chen[5], Gianni Ciavarra[1,4], Alessandro Datti[6], Tak W. Mak[5], Lea Harrington[7], Fred Dick[8], Gary D. Bader[2], Rod Bremner[3,4], Minna Woo[1,9] and Eldad Zacksenhaus[1, 4, 9, *]

I. METHODS

II. LEGENDS TO SUPPLEMENTARY FIGURES

III. REFERENCES TO SUPPLEMENTARY DATA

IV. FIGURES:

I. METHODS

Generation, genotyping and analysis of knock-in mice

Targeting vectors were constructed using genomic DNA from 129/sv mice, and standard techniques (supplemental Figure S1A). In brief, an Xba1-BamH1 fragment of 7.8KB, spanning exon intron 18 to intron 22 was sub-cloned into a modified pBS vector with a NotI at its 3' end (pBS-Rb2). A BamH1-EcoRV fragment flanking exon 23 was subcloned into a modified pBS vector (pBS-BamH1-RV.X23ΔK4/7), and the Ser/Thr sites were mutagenized to Ala residues by PCR-mediated site-specific mutagenesis. Specific mutations were verified by sequening. A fragment spanning exon 24 from EcoRV to BamH1 in intron 24 was subsequently subcloned into pBS-BamH1-RV.X23ΔK4/7, and a loxP_pgk.neo_loxP cassette was inserted at the EcoRV sites as an EcoRV-Sma1 fragment, yielding pBS-BamH1-RV-.X23ΔK4/7/lox. The latter was introduced into pBS-R2 as a BamH1-Not1 fragment resulting in the targeting vectors shown in supplemental Figure S1C. Additional details available upon request.

$Rb^{\Delta K4.neo}$ and $Rb^{\Delta K7.neo}$ targeting vectors were electroporated into ES cells and approximately 200 G418-resistant clones were screened by Southern blot hybridization analysis with a radioactive DNA probe located 3' downstream of the vector DNA using probes shown in supplemental Figure S1B. Four and twenty putative clones, respectively, that produced the expected 3.5 Kb knock-in DNA fragment in addition to the 6.5Kb wild-type band were identified in the initial screens. Two clones were further confirmed by Southern blots with *5'*, *neo* and *3'* probes using multiple restriction enzymes to have undergone the desired homologous recombination. As the Xba1-Xba1 5' probe contains abundant repeats at the 5' end, we generated a unique probe from the 3' end by PCR as shown in Figure S1A. These were verified with additional restriction enzymes as well as 5' and neo probe.

Subsequent genotyping was performed by PCR analysis of tail DNA. Primers a - b (Fig. S1B): a 5'-GTAACCATACTGCAGCAG; b 5'-TTGGAGAT-CTTAGAGGAG. Protamine.Cre mice were obtained from JAX and identified by PCR using primers for Cre: 5'-TCGCGATTATCTTCTATATCTTCAG and 5'-GCTCGACCAGTT TAGTTACCC. Mice used for experiments were genotyped twice from two independent biopsies.

$Rb^{23A4neo}$:Rb^{wt} and $Rb^{23A7neo}$:Rb^{wt} chimeric mice were generated and crossed with C57B6/L or 129/sv mice. Progeny were screened for germ-line transmission by Southern blots and PCR analyses to identify $Rb^{23A4neo/+}$ and $Rb^{23A7neo/+}$ mice. To remove the floxed pgk.neo cassette, $Rb^{23A4.neo}$ mice were mated with Protamine.Cre mice, in which the Cre recombinase is expressed in spermatids (O'Gorman *et al*, 1997). Male $Rb^{23A4neo}$:Prot.Cre mice were crossed with C57B6/L females and progenies, referred to as $Rb^{\Delta K4/+}$ mice, which have lost the Pgk.*neo* cassette but retained a single loxP site, were detected by PCR. To confirm the Rb^{23A4} and $Rb^{23A7.neo}$ sequence, the DNA region flanking exon 23 including the 5' and 3' boundaries (using primers I and III in Fig. S1B) were amplified by PCR, sub-cloned into pBluescript and sequenced. The targeted Ser/Thr-to-Ala substitutions but not unwanted mutations were confirmed (not shown). Mice were analyzed as described (Jiang *et al*, 2010) (Cai *et al*, 2012). Vitamin C (L-ascorbyl-2-polyphosphate) supplemented chow (1%) was obtained from Harlan, and used to feed heterozygous $Rb^{\Delta K7/+}$ breeding pairs and then their progeny for the indicated duration.

Isolation and differentiation of myoblasts and immunofluorescence

Primary myoblasts were isolated from limb muscles of E16.5 embryos under a dissecting microscope as described (Ciavarra & Zacksenhaus, 2010). Single cells were obtained by repeated

tituration with a Pasteur pipette after incubating with 0.25% trypsin/EDTA and 300 units/ml collagenase II (Sigma) at 37°C water bath for 30 minutes. Primary cells were cultured in growth media (GM), containing 1:9 DMEM:HAM-F10 media (Sigma), supplemented with 20% fetal bovine serum (Hyclone) in 5% CO_2, 37°C incubator. Myoblast cultures were further enriched by differential plating: the cells were seeded into poly-L-lysine (Sigma) coated plates to allow fibroblasts to adhere for 30 minutes at 37°C and none adherent myoblasts were recovered. Primary myoblasts were used at passage 2-3.

At confluency, primary myoblasts were induced to differentiate on collagen-I coated coverslips (BD Biosciences) by removing the growth medium and replacing with DMEM (Sigma) containing 2.5% horse serum (HyClone) and penicillin-streptomycin (Sigma). At the desired time-point, cells were fixed with 2% PFA, permeabilized with 0.3% Triton X-100 and blocked using 1% BSA in PBS at room temperature. Cells were stained using antibodies against skeletal myosin heavy chain (clone MY-32) at a dilution of 1:50. Fluorescein-conjugated (Alexa Fluor 488) (Molecular Probes) secondary antibodies were added for 45min. Nuclei were counterstained with DAPI (Molecular Probes) for 10min and cells were mounted in fluorescent mounting media (Dako). Fluorescent images were viewed using Axioskop2 fluorescent microscope (Carl Zeiss Inc.) and LSM 510 confocal microscope (Carl Zeiss Inc.) and digitally acquired using an AxioCam MRc (Carl Zeiss Inc.) at room temperature. Photoshop CS (Adobe) was used to overlay images.

BrdU and flow cytometry analysis of T cells

Thymus, spleen or lymph nodes were dissected into 1% BSA/PBS and single cell suspension was made by mincing between two slides and passing through 40μ cell strainer followed by multiple passage through 10 ml pipettes. The cells were counted and $1x10^6$ cells were incubated with CD4-FITC (Cat. No: 554837, Clone: OX-35), CD8a-PE (Cat. No.: 553032, Clone: 53-6.7), CD3e-Biotin (Cat. No.: 550395, Clone: 145-2C11), all from BD Biosciences, for 2hr, washed and (for biotinylated Ab) treated with streptavidin-PerCP-Cy5.5 second Abs (Cat. No.: 551419, BD Biosciences) for 30 min, followed by washing and analysis by FACSCalibur flow cytometer (BD Biosciences, San Jose, CA) as described (Ho *et al*, 2007).

Bone marrow-derived macrophages and TLR ligands stimulation

Single cell suspensions were prepared from mouse bone marrows as described (Chen *et al*, 2008). Red blood cells were removed from spleens by incubating suspended cells in sterile ACK buffer (0.155mM ammonium chloride, 0.1mM disodium EDTA, 0.01M potassium bicarbonate) for 5 minutes on ice. After washed with RPMI medium plus 10% FBS and 2-ME, cells were counted and replated in 10 cm tissue culture plates ($5x10^6$/plate in 6ml 10%FBS RPMI medium with 2-ME and 25ng/ml M-CSF). Three ml fresh medium with M-CSF was added into each plate every other day. The cells were washed and harvested at day 5 in ice cold PBS with 10 mM EDTA. Cells were then counted and replated onto flat bottom 96 well culture plate at 10^5/well for 4 hours and then stimulated with indicated concentrations of LPS, LTA, PGN and polyIC (all obtained from Sigma) for 24 hours. Supernatants were then harvested and IL-6 concentrations were determined using ELISA EIA from BD-bioscience.

II. LEGENDS TO SUPPLEMENTARY FIGURES

Fig. S1. Normal myogenesis in $Rb^{\Delta K4}$ and $Rb^{\Delta K7}$ mice.
A. Apparent normal skeletal myogenesis in $Rb^{\Delta K4}$ mice. Left, MHC staining of transverse sections through skeletal muscles of E16.5 $Rb^{\Delta K4}$ or control embryos. Right, MHC staining of myoblasts isolated from indicated embryos and induced to differentiate into myotubes *in vitro*.
B. Apparent normal skeletal myogenesis in $Rb^{\Delta K7}$ mice. Left, Troponin T staining of skeletal muscles from E16.5 $Rb^{\Delta K7}$ and control littermates, Right, differentiation of $Rb^{\Delta K7}$ myoblasts to form myotubes expressing MHC and CyclinD3. $Rb^{\Delta K7}$ myotubes also twitched like control fibers (not shown).

Fig. S2. Telomere attrition in $Rb^{\Delta K4}$ splenocytes
A. Quantitative analysis of metaphase spreads from 5 pairs of splenocytes from $Rb^{\Delta K4}$ and control littermates hybridized with a telomere repeat probe (Two-tailed Mann-Whitney-Wilcoxon test $P<0.001$). Related to Fig. 1D.
B. GST-suv4-20h1 and GST-suv4-20h2 pull down of unphosphorylated pRb from protein lysates from normal wildtype thymocytes. Empty GST vector and GST-E1a were used as negative and positive controls. Wild-type and $Rb^{\Delta K7}$ lysates were run in parallel to indicate hypo- and hyper-phosphorylated pRb species.

Fig. S3. Near normal hematology in $Rb^{\Delta K7}$ mice. Blood samples from 8 (top) and 22 (bottom) week $Rb^{\Delta K7}$ mice were analyzed using VetSCan HM5 V2.31 analyzer. No hematological differences were detected in a total of 15 $Rb^{\Delta K7}$ and control mice.

Fig. S4. Near normal response of bone marrow (BM) macrophages from $Rb^{\Delta K7}$ mice to Toll-like ligands *in vitro*
IL6 levels in bone marrow (BM) macrophages from $Rb^{\Delta K7}$ and control wildtype mice in response to indicated Toll-like ligands *in vitro*. * denotes a $Rb^{\Delta K7}$ mouse with kyphosis. Similar results were obtained in two independent experiments.

Fig. S5. Increased expression of SOX9 and PDX1 but no detectable expression of Kir6-2 in $Rb^{\Delta K7}$ islets
A. Increased staining of SOX9 in ductal epithelial and centroacinar cells in $Rb^{\Delta K7}$ pancreas relative to control littermates. No such increase in staining was observed in pancreatic islets (not shown).
B. Increased nuclear PDX1 staining in $Rb^{\Delta K7}$ islets relative to control littermates.
C. Representative IHC for Kir6-2 showing no detectable expression in $Rb^{\Delta K7}$ vs. control islets.

Fig. S6. Immunostaining analysis for DDR-related factors in $Rb^{\Delta K7}$ islets and immunoblots for Thr350 expression in Vitamin C fed $Rb^{\Delta K7}$ vs control mice
A. Double immunofluorescent staining for gH2A and BrdU of pancreatic islets in $Rb^{\Delta K7}$ vs control mice. $Rb^{\Delta K7}$ islet show multiple γH2A positive nuclei that do not stain for BrdU indicating that cells are not in proliferating phase.

B. Immunostaining for phospho-Ser1981-ATM and phospho-ATR-substrates in $Rb^{\Delta K7}$ vs control islets. Inlets depict high magnification of cells with punctate staining (arrows).
C. Left, immunostaining analysis for p53BP1. Arrows indicate cells with intense staining shown at high power in inlets in $Rb^{\Delta K7}$ islets. Right, average fraction of islets with strong nuclear p53BP1 staining.
D. Left, immunostaining analysis for H3K9me3. Arrows indicate nuclei with intense staining, shown at high power in inlets in $Rb^{\Delta K7}$ islets. Right, average fraction of islets with strong nuclear H3K9me3 staining.
E. Immunostaining analysis for HP1γ, phospho-Ser15-p53 and H3K27me3 showing no obvious difference between $Rb^{\Delta K7}$ and control islets.
F. Vitamin C does not induce phosphorylation of RbΔK7 on Thr350. Western blot analysis of control and RbΔK7 thymocytes from mice fed on regular chow or vitamin C diet, using antibody for Thr350. Actin was used as loading control. n.s. denotes a non-specific, cross reactive band.

III. REFERENCES FOR SUPPLEMENTARY DATA

Cai EP, Casimir M, Schroer SA, Luk CT, Shi SY, Choi D, Dai XQ, Hajmrle C, Spigelman AF, Zhu D *et al* (2012) In vivo role of focal adhesion kinase in regulating pancreatic beta-cell mass and function through insulin signaling, actin dynamics, and granule trafficking. *Diabetes* 61: 1708-1718

Chen NJ, Chio, II, Lin WJ, Duncan G, Chau H, Katz D, Huang HL, Pike KA, Hao Z, Su YW *et al* (2008) Beyond tumor necrosis factor receptor: TRADD signaling in toll-like receptors. *Proc Natl Acad Sci U S A* 105: 12429-12434

Ciavarra G, Zacksenhaus E (2010) Rescue of myogenic defects in Rb-deficient cells by inhibition of autophagy or by hypoxia-induced glycolytic shift. *J Cell Biol* 191: 291-301

Ho AT, Li QH, Okada H, Mak TW, Zacksenhaus E (2007) XIAP Activity Dictates Apaf-1 Dependency for Caspase9 Activation. *Mol Cell Biol*

Jiang Z, Deng T, Jones R, Li H, Herschkowitz JI, Liu JC, Weigman VJ, Tsao MS, Lane TF, Perou CM *et al* (2010) Rb deletion in mouse mammary progenitors induces luminal-B or basal-like/EMT tumor subtypes depending on p53 status. *J Clin Invest* 120: 3296-3309

O'Gorman S, Dagenais NA, Qian M, Marchuk Y (1997) Protamine-Cre recombinase transgenes efficiently recombine target sequences in the male germ line of mice, but not in embryonic stem cells. *Proc Natl Acad Sci U S A* 94: 14602-14607

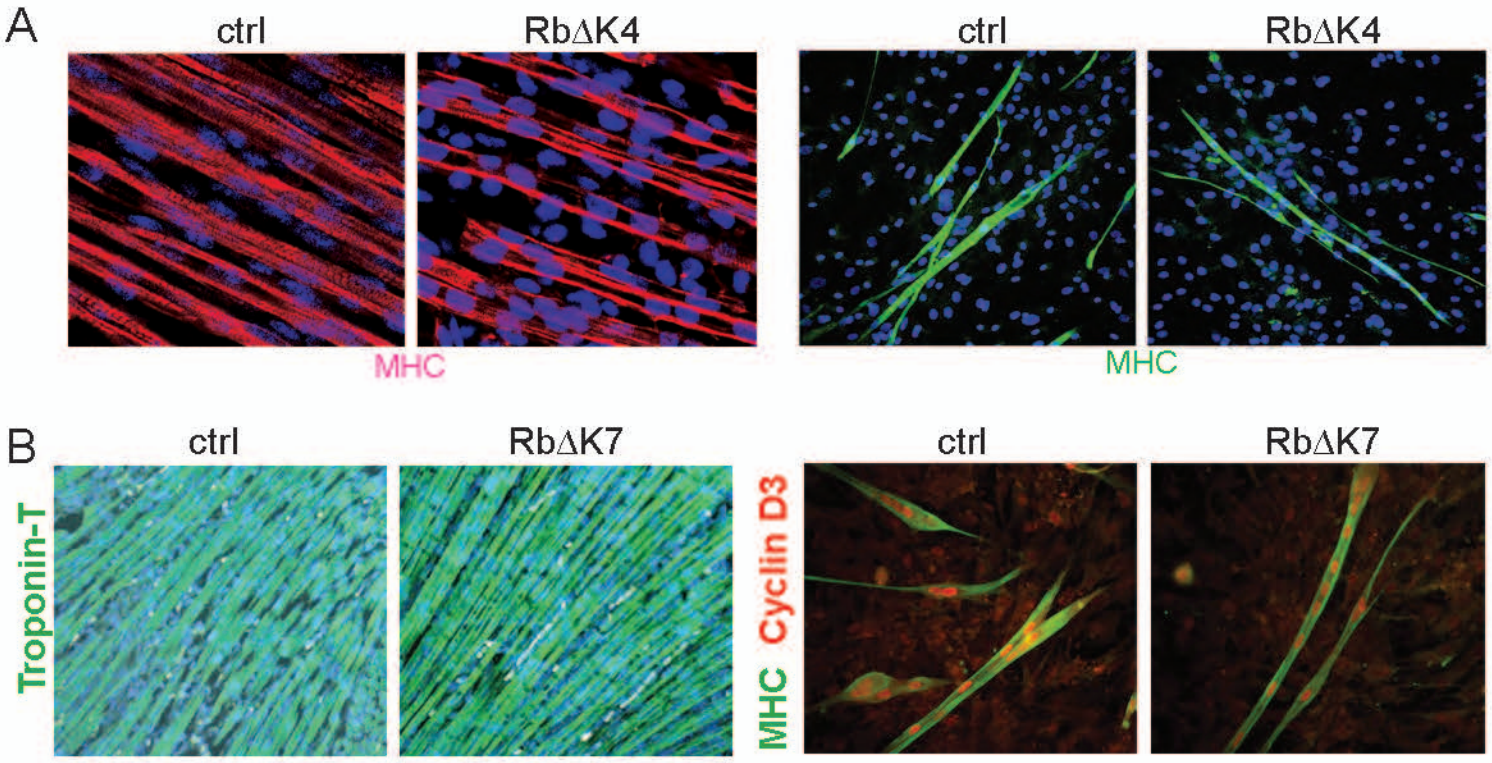

Appendix Fig. S1

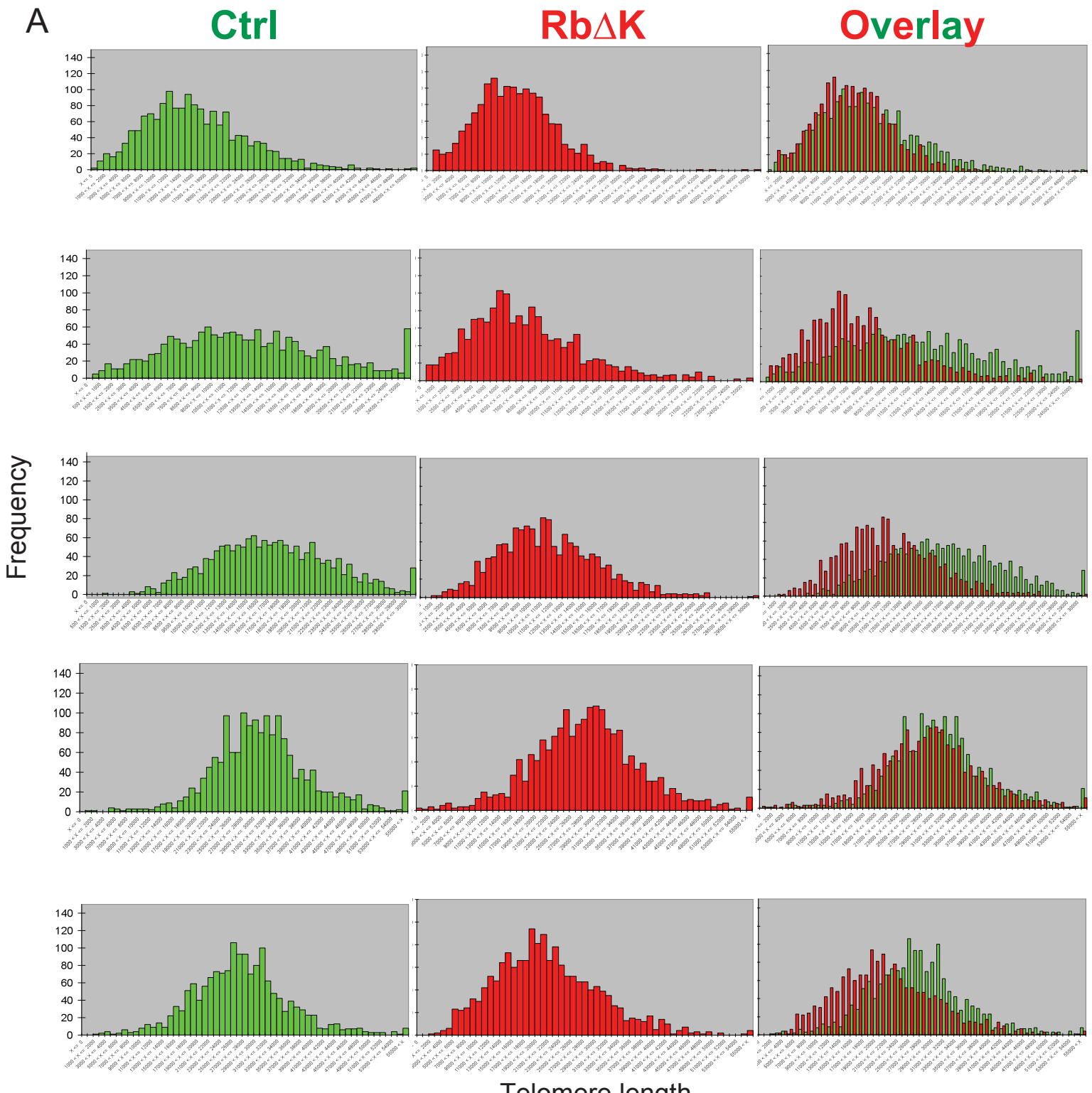

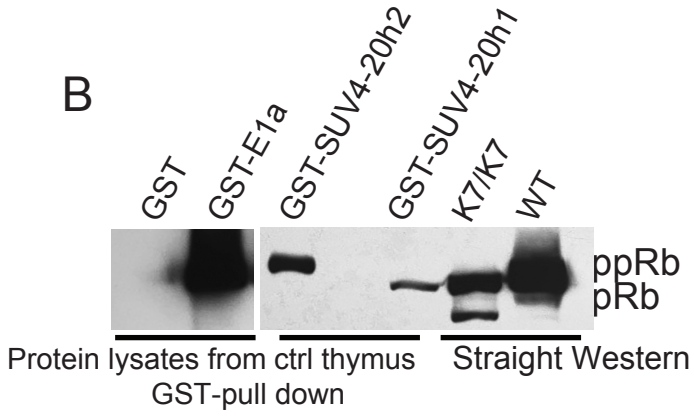

Appendix Fig. S2

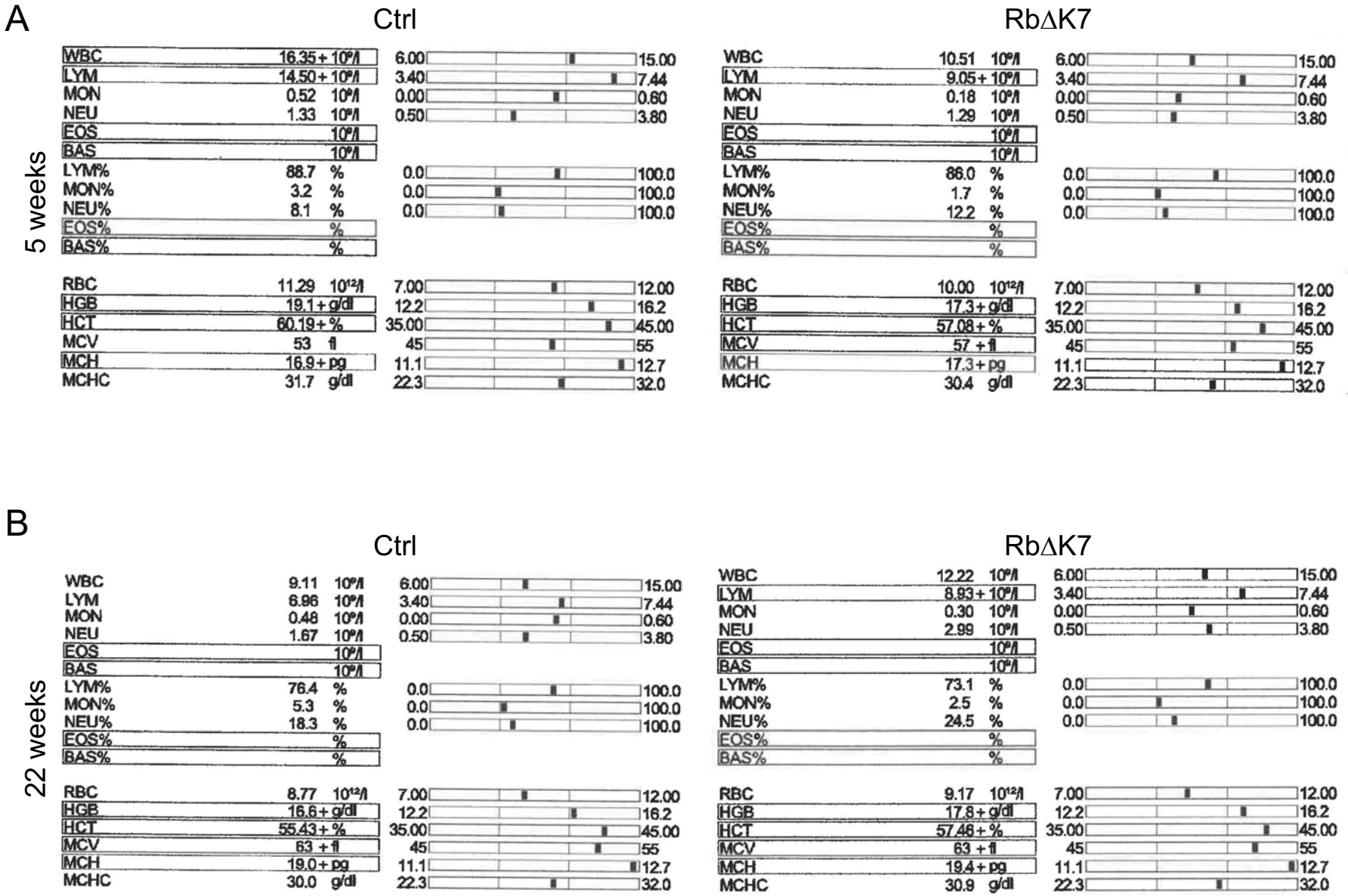

Appendix Fig. S3

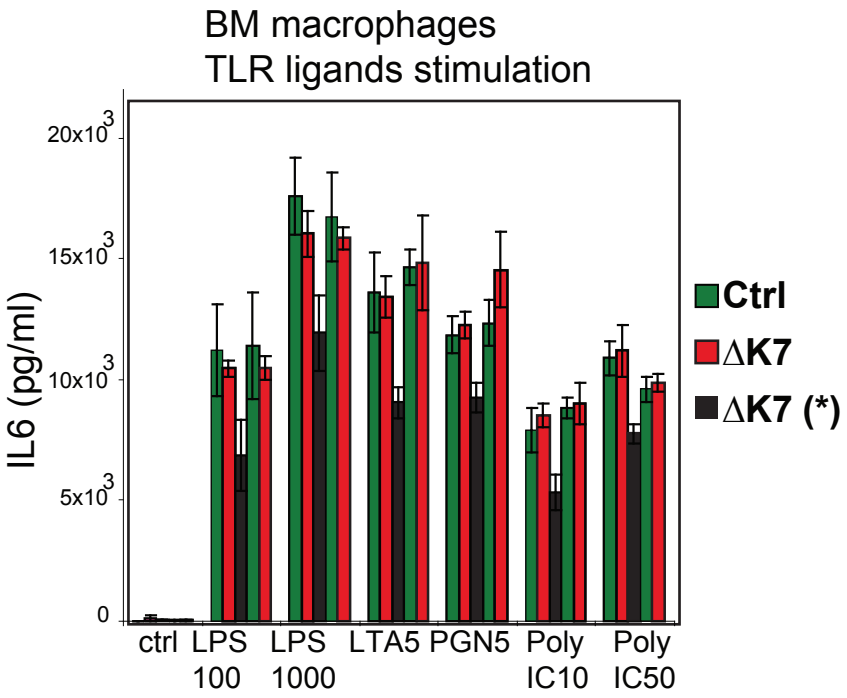

Appendix Fig. S4

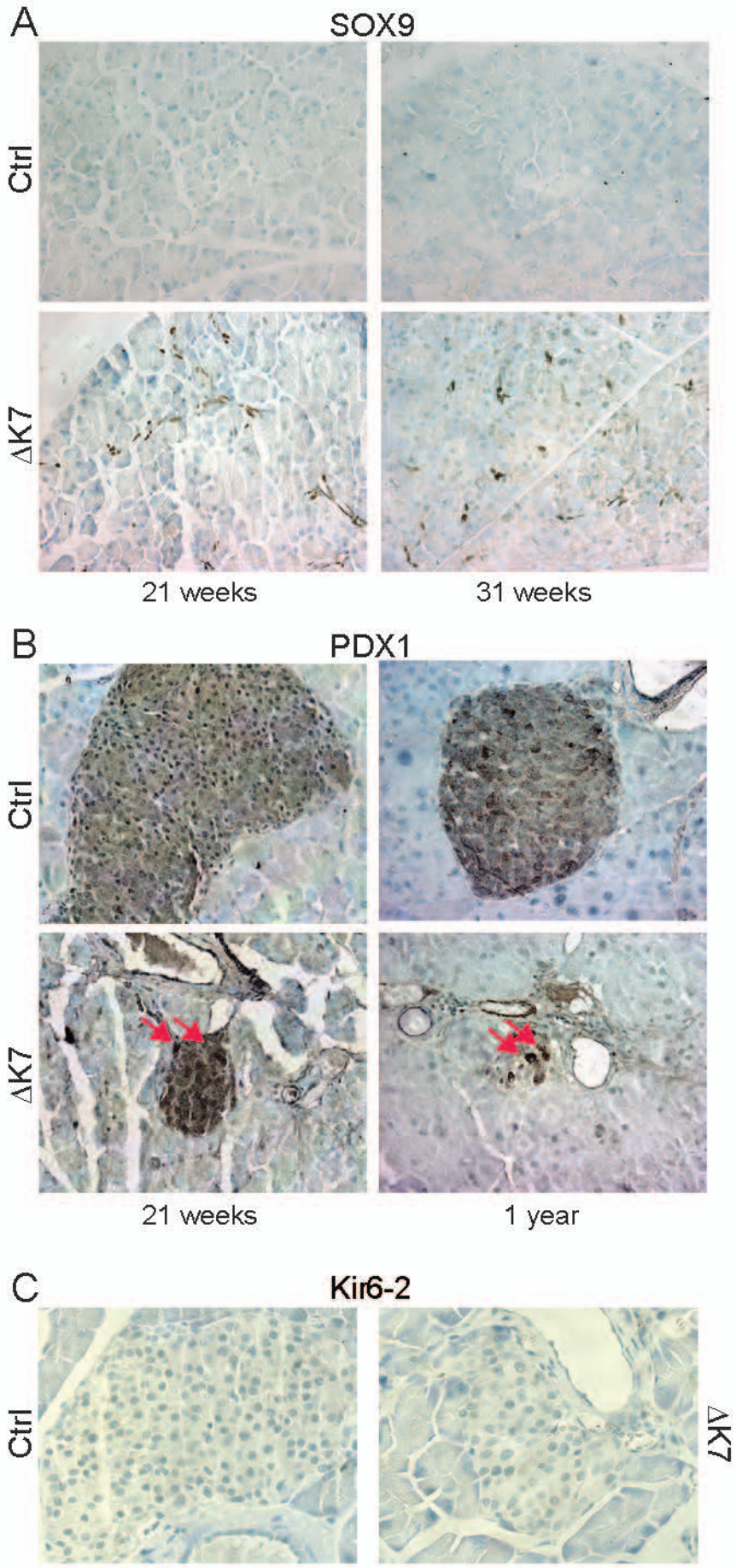

Appendix Fig. S5

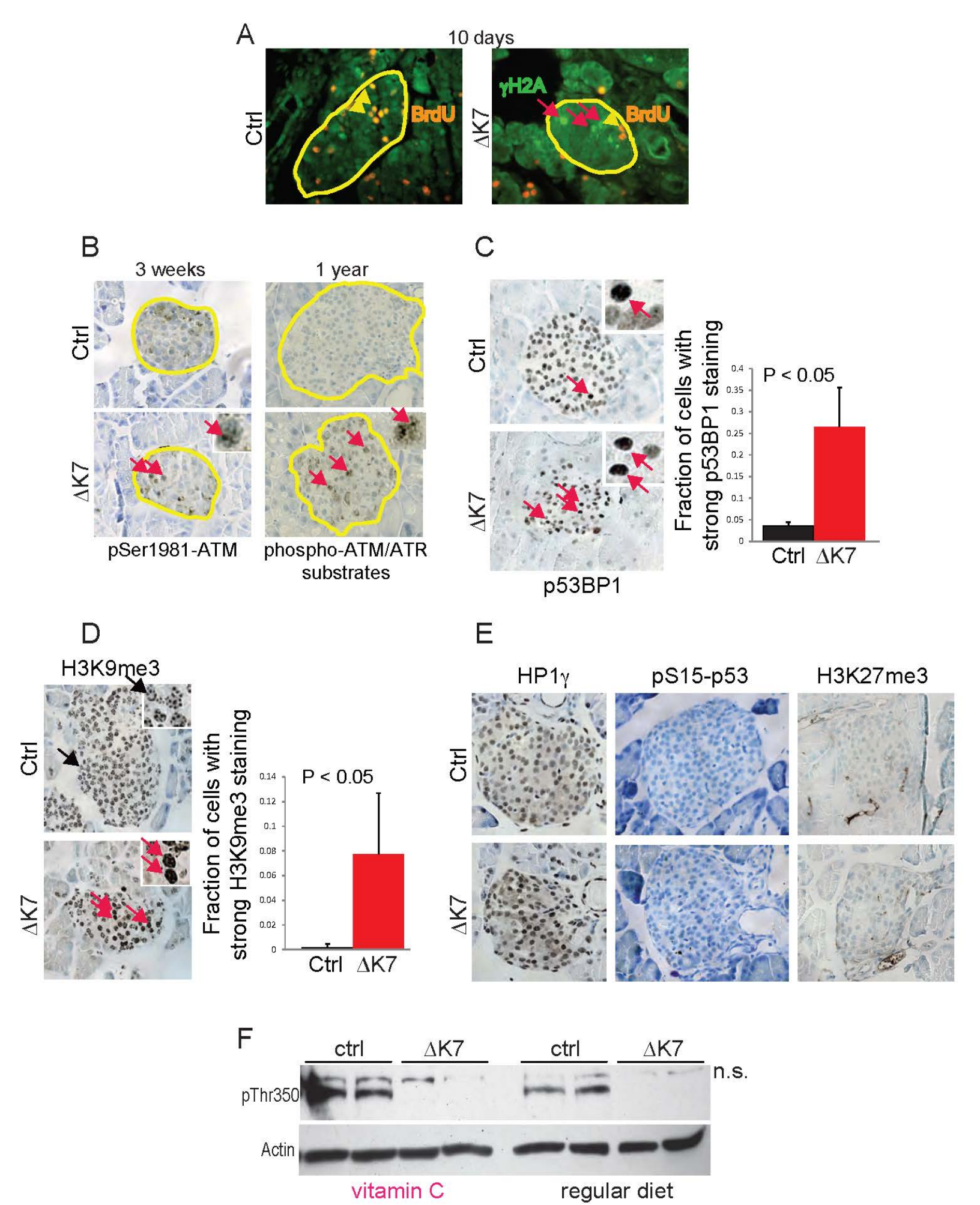

Appendix Fig. S6